Journal of Southeast University (English Edition) Vol. 27, No. 4, pp. 452 – 457 Dec. 2011 ISSN 1003—7985

Influence of dye molecular structure on electron transfer in 2, 9, 16, 23-tetracarboxy zinc phthalocyanine sensitized solar cell

Wang Yuqiao[1] Cui Xia[1] Ma Yiwen[1] Qi Haonan[1] Zhang Huijun[1]
Zhang Yuan[2] Sun Yueming[1]

([1]School of Chemistry and Chemical Engineering, Southeast University, Nanjing 211189, China)
([2]School of Chemistry and Chemical Engineering, Yangzhou University, Yangzhou 225002, China)

Abstract: 2, 9, 16, 23-tetracarboxy zinc phthalocyanine (ZnTCPc) is synthesized and characterized by physicochemical and theoretical methods and it is used as a photosensitizer in dye-sensitized solar cells (DSSC). The excited lifetime, band gap and frontier orbital distribution of ZnTCPc are investigated by fluorescence spectra, cyclic voltammetry and quantum calculation. The results show that the excited lifetime and band gap are 0.1 ns and 1.81 eV, respectively. Moreover, it is found that the highest occupied molecular orbital (HOMO) location is not shared by both the zinc metal and the isoindoline ligands, and the lowest unoccupied molecular orbital (LUMO) location does not strengthen the interaction coupling between ZnTCPc and TiO_2. As a result, the ZnTCPc-DSSC gains a short-circuit current density of 0.147 mA/cm^2, an open-circuit photovoltage of 277 mV, a fill factor of 0.51 and an overall conversion efficiency of 0.021%.

Key words: zinc phthalocyanine; solar cell; frontier orbital; electron transfer
doi: 10.3969/j.issn.1003 – 7985.2011.04.021

Dye-sensitized solar cells (DSSC) have attracted much attention due to low cost and high efficiency[1]. The key operation of the DSSC is based on ultrafast photoinduced electron injection from the sensitizer into the conduction band (CB) of the oxide semiconductor. So far, ruthenium polypyridyl dyes have been proved to be effective sensitive dyes for the DSSC, such as $Ru(bpy)_2(NCS)_2$ (N3), $(Bu_4N)_2$-Ru(dcbpyH)$_2$(NCS)$_2$ (N719), and Ru$(H_3tcterpy)(SCN)_3(C_2H_5)_3NH$ (black dye)[2]. These Ru-dyes comply with several requirements as follows: First, the Ru-dyes have the light-harvesting capacity and the anchoring group to gain light energy and be adsorbed on TiO_2 surface, respectively. Secondly, their lowest unoccupied molecular orbital (LUMO) energy level is higher than the TiO_2 CB energy level, which ensures the photoelectron injection from the excited dyes into the CB edge. Thirdly, their highest occupied molecular orbital (HOMO) energy level is lower than the redox energy level, which ensures regeneration from the oxidized state of Ru-dyes to the reduced state. Though a conversion efficiency of 11% has been achieved in Ru-dye DSSCs[3], ruthenium is a scarce resource and its complexes lack near-IR absorption. Considering the cost, stability and near-IR light-harvesting, phthalocyanine is one of the most promising sensitizers. However, most of phthalocyanine-sensitized solar cells exhibit poor performance, owing to strong aggregation, poor solubility and lack of directional electron transfer in the excited state[4–5]. Since it is very difficult to calculate and demonstrate all the necessary parameters in the DSSC system, the typical problems should be solved preferentially, such as frontier orbital locations, energy level distributions and their relationships to photovoltaic properties. Nonetheless, the influence factors of the device performance can be conformed by the spectral, electrochemical and quantum calculation methods.

In this paper, 2, 9, 16, 23-tetracarboxy zinc phthalocyanine (ZnTCPc) is synthesized by ammonium molybdate solid phase catalysis. Compared with the N3-DSSC, the performance of ZnTCPc-DSSC is investigated by experimental and theoretical analysis, such as the light absorbance, the excited electron state lifetime, the dark current, the energy level distribution and the frontier orbital location.

1 Experimental Section

1.1 Material and methods

The TiO_2 powder and fluorine-doped tin oxide transparent glass (FTO, sheet resistance 10 Ω/cm^2) were purchased from Degussa and Asahi. All other reagents from Aldrich were used without further purification. Elemental analysis was monitored by Perkin-Elmer240C. IR, UV-vis, fluorescence emission and decay spectra were characterized by Nicolet750, Shimadzu2201 and Edinburgh900. The cyclic voltammetry (CV) of ZnTCPc was carried out on a CHI660B electrochemical workstation with the platinum working electrode, platinum counter electrode and Ag/Ag-NO_3 reference electrode. The electrode potential was calibrated with respect to the ferrocene/ferrocenium (Fc/Fc^+) couple. The CV experiments were performed in a dry box under N_2 atmosphere at room temperature. Photovoltaic properties were measured by Keithley under Oriel solar simulator (AM1.5, 100 mW/cm^2) illumination. Equipped

Received 2011-05-31.
Biography: Wang Yuqiao (1977—), male, doctor, associate professor, yqwang@seu.edu.cn.
Foundation items: The National Natural Science Foundation of China (No. 21173042), the National Basic Research Program of China (973 Program) (No. 2007CB936300), the Natural Science Foundation of Jiangsu Province (No. BK201123694), Foundation of Jiangsu Key Laboratory of Environmental Material and Environmental Engineering (No. JHCG201012), Foundation of Key Laboratory of Novel Thin Film Solar Cells of Chinese Academy of Sciences (No. KF200902), Science and Technology Foundation of Southeast University (No. KJ2010429).
Citation: Wang Yuqiao, Cui Xia, Ma Yiwen, et al. Influence of dye molecular structure on electron transfer in 2, 9, 16, 23-tetracarboxy zinc phthalocyanine sensitized solar cell[J]. Journal of Southeast University (English Edition), 2011, 27(4): 452 – 457. [doi: 10.3969/j.issn.1003 – 7985.2011.04.021]

with a monochromator, IPCE was measured.

1.2 Preparation and structure of ZnTCPc

Dehydrated zinc chloride of 4.1 g, trioctyl trimellitate (TOTM) of 10.6 g and ammonium molybdate of 0.8 g were ground in an agate mortar. The mixture with urea of 40 g was heated to 150 ℃ with vigorous stirring. These pastes were maintained at 150 ℃ for 1 h and then at 200 ℃ for 1 h until the viscous blue pastes were obtained. After cooling to room temperature, the blue powder was ground into fine particles and refluxed with 2 mol/L hydrochloric acid for 24 h. The foaming precipitates were collected by hot filtration, washed by ethanol and dried at 120 ℃. The dry precipitates of 1.0 g were refluxed in a 0.5 mol/L potassium hydroxide aqueous solution for 24 h. Finally, the pH value of the mixed solution was adjusted to 6 by hydrochloric acid.

Elemental analysis of $C_{36}H_{16}N_8O_6Zn$ (MW 753.97) was performed. Experimental: C 52.59%, H 3.12%, N 16.22%; calculated: C 54.73%, H 2.55%, N 14.18%. IR spectra (cm^{-1}): 3 352 (s, OH-carboxylic acid), 1 697 (s, CO-arylcarboxylic acid), 1 611 (s, C═Caryl), 1 520 (CN-conjugated cyclic system), 1 336 (m), 1 086 (w). Uv-Vis spectra (nm, in DMSO): 688, 619 and 345.

1.3 Computational methods

The frontier orbital localization of ZnTCPc was calculated by the density functional theory (DFT) using Gaussian 98 which ran on a Pentium IV PC. The geometries of the ZnTCPc molecule were optimized with the B3LYP functional and the 3-31G(D) basis set.

1.4 DSSC fabrication

TiO_2 of 6.0 g, glacial acetic acid of 12 g, ethyl cellulose of 2.0 g, polyethylene glycol of 2.0 g and Triton X-100 of 0.1 mL were mixed and ground in a mortar. The slurry was spread onto FTO substrate through screen-printing. After sintering at 450 ℃ for 30 min and cooling to 80 ℃, the TiO_2 film electrode was immersed in the saturated ZnTCPc/DMSO solution overnight. The electrolyte consisted of 0.5 mol/L lithium iodide, 0.05 mol/L iodine and 0.5 mol/L 4-tertbutylpyridine in propylene carbonate. The sandwich device with an active area of 0.20 cm^2 included ZnTCPc-sensitized TiO_2 film electrode, electrolytes and platinized FTO counter electrode.

2 Results and Discussion

2.1 Spectra and electrochemical properties of ZnTCPc

It is well-known that the absorption spectrum of N3 is dominated by metal to ligand charge transfer (MLCT) transitions in the visible region with the lowest allowable MLCT bands appearing at 385 and 530 nm[6]. As shown in Fig. 1 (a), ZnTCPc has typical B-band (279 nm) and Q-band (619 and 688 nm) absorption. Generally, Q-band absorption is assigned as MLCT transition to absorb the near-IR solar radiation[7]. After ZnTCPc is absorbed by TiO_2 film electrodes, the absorption bands shift from 688 to 703 nm, and furthermore, the corresponding peaks appear to be broad in TiO_2 films. The absorbed bands of monomer and dimer shift towards the long wavelength region. The results indicate that the LUMO energy level of ZnTCPc is lower than that of N3. However, the dimeric peak still exists, locating at 635 nm. The excess of dimers are absorbed on TiO_2 surface as a filter, decreasing the light-harvesting and hindering the injecting electrons transfer from excited dyes to semiconductors.

The emission peak (685 nm) of ZnTCPc shown in Fig. 1(b) is obtained at room temperature in DMSO solvent. Interestingly, the quenched emission spectrum is observed when the ZnTCPc is adsorbed onto TiO_2 layer as a consequence of electron injection from the excited state of ZnTCPc into the CB of TiO_2[8]. The phenomena can be explained by the efficient electron injection from the excited singlet state of phthalocyanines to the semiconductor CB[9]. Both the broadened UV-vis absorbance and the quenched emission indicate strong interactions between the ZnTCPc and TiO_2 film surfaces. The above results prove that ZnTCPc-sensitized TiO_2 electrodes are suitable for DSSC in terms of the light absorbance and the electron injection.

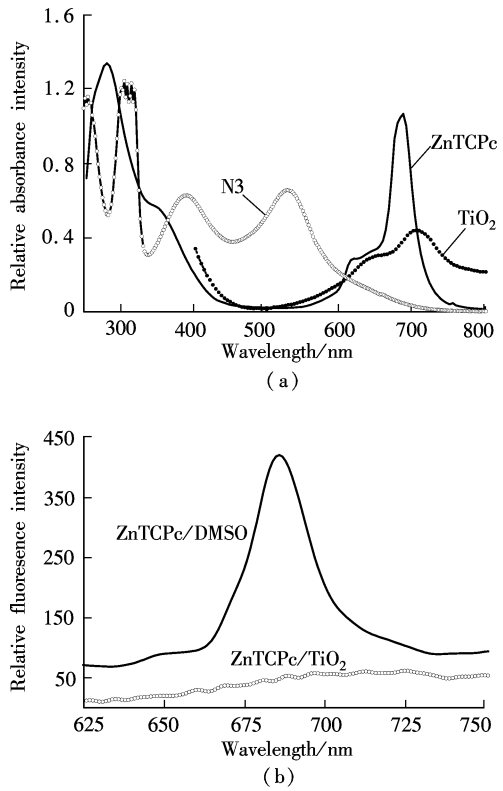

Fig. 1 Spectra comparison. (a) UV-vis; (b) Fluorescence emission

The CV data can evaluate the energy levels of HOMO (E_{HOMO}) and the energy levels of LUMO (E_{LUMO}) with the help of the maximum UV-vis absorption of dyes. As shown in Fig. 2(a), CV curves offer us only one oxidation peak (0.99 V vs. $Ag/AgNO_3$, pointed by the arrow). The absorption onset of ZnTCPc is used to calculate the energy gap E_g, E_{HOMO} and E_{LUMO} as follows:

$$E_{HOMO} = E_{ox} - E_{Fc/Fc^+} + 4.8 \quad (1)$$

$$E_g = \frac{1\,240}{\lambda_{max}} \quad (2)$$

$$E_{LUMO} = E_{HOMO} - E_g \quad (3)$$

where E_{ox} is the oxygen potential of ZnTCPc and λ_{max} is the absorption threshold (λ_{max} = 688 nm) of ZnTCPc in the DMSO solution. To thermodynamically judge the possibility of electron transfer from the excited dye to the CB of TiO_2, the E_{HOMO} and E_{LUMO} of ZnTCPc can be established from the spectral and electrochemical properties. The corresponding data are summarized in Tab. 1.

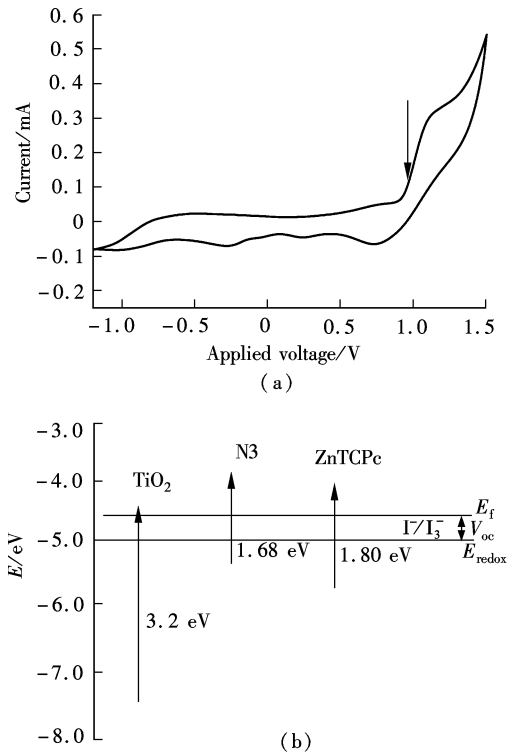

Fig. 2 Potential and energy diagrams. (a) CV results; (b) Energy level

Tab. 1 Data of ZnTCPc absorption spectra and electrochemistry

Sample	Absorbance peak/nm			E_{HOMO}/eV	E_{LUMO}/eV	E_g/eV
N3[6]	311	385	530	−5.52	−3.84	1.68
Experimental	279	619	688	−5.79	−3.99	1.80
Theoretical				−5.52	−3.24	2.28
Ref. [10]			680	−6.21	−4.40	1.81

From the present data, no function can be assigned to the oxidation of the metal center or the oxidations of the macrocycle in ZnTCPc molecule. If one or more zinc redox processes occur at potentials lying between the ZnTCPc oxidation and reduction, we may infer that one or more zinc d levels lie between the ZnTCPc HOMO and LUMO orbitals. So we cannot clearly confirm that the excitation of ZnTCPc involves transfer of an electron from the metal to the π^* orbital of the ligand until the position of a zinc d level is confirmed. According to Tab. 1, the scheme of energy levels of DSSC is described as a thermodynamical process in Fig. 2 (b). The E_{HOMO} and E_{LUMO} of ZnTCPc match the energy levels of TiO_2 and the potential of I^-/I_3^- redox couples. The lower the E_{LUMO} of ZnTCPc excited state is, the more difficult the electron-transfer reaction. The more the negative E_{HOMO} is, the better the dye regeneration by electron donation from I^-/I_3^-.

Previously, theoretical investigations on N3 have mainly been performed by means of semiempirical, DFT and ZINDO/1 calculations[10-11]. In Fig. 3, atoms in red, gray, white, blue and lilac correspond to oxygen, carbon, hydrogen, nitrogen and zinc, respectively. The HOMO location is not distributed on the zinc metal but is distributed on the isoindoline ligands. Correspondingly, the HOMO − 1 location has amplitudes on the zinc metal and inner rings. The result suggests that the HOMO level is not actually shared by both the zinc metal and the isoindoline ligands. Obviously, the symmetry structures of ZnTCPc cause a low dipole moment for the transition from Zn-2, 9-tetracarboxylic orbitals to the 16, 23-tetracarboxylic orbitals, which induces an unfavorable MLCT transition. Analogously, LUMO and LUMO + 1 are localized homogeneously in the whole molecular, but do not focus on the carboxylic groups. In other words, the large-scale participation to the LUMO and LUMO + 1 orbitals may reduce the interaction coupling between the dye and the semiconductor. The phenomena indicate that the interaction coupling between ZnTCPc and TiO_2 has been weakened; that is to say, the zinc d levels do not make a contribution to the MLCT process of ZnTCPc. The low efficiency of injecting electrons will not contribute to an excellent DSSC characterization. On the contrary, LUMO and HOMO in N3 have each undertaken obvious functions[11]. On the one hand, the NCS ligands share the HOMO with Ru metal; especially the NCS groups inserting the electrolyte may facilitate reduction by I^-. On the other hand, the bpy rings share the LUMO with the COOH groups, ensuring electron transfer from the excited state to the conductor band of TiO_2. Considering the above-mentioned analysis, the frontier orbital locations of N3 help the electron injection and dye regeneration further.

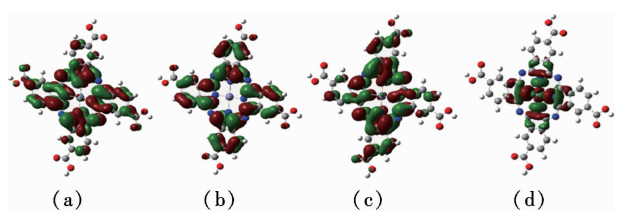

Fig. 3 Distribution of frontier orbitals. (a) LUMO; (b) HOMO; (c) LUMO + 1; (d) HOMO − 1

In terms of kinetics and mechanism, the conversion efficiency is also influenced by the electron injection rate and the recombination rate. The fluorescence decay of ZnTCPc shows a nonexponential behavior in Fig. 4. It can be estimated that the excited state lifetime of ZnTCPc is around 0.1 ns. Obviously the rate of electron injection should be much faster than that of the fluorescence decay of the sensitizer dye. While N3 emits at 750 nm, the excited state lifetime is 60 ns[11]. Under the same condition

of electron trapping within the defect/surface states of the TiO_2 film, the recombination rate of the ZnTCPc-sensitized TiO_2 film must be greater than that of the N3-sensitized TiO_2 film[12]. As a result, the photocurrent of DSSC drops sharply and the corresponding overall conversion efficiency η behaves badly.

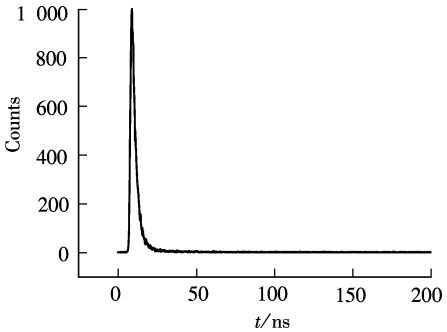

Fig. 4 Fluorescence decay spectra for ZnTCPc in DMSO solution

2.2 Photovoltaic performance

The photovoltaic properties of ZnTCPc-DSSC and N3-DSSC are shown in Tab. 2. The formulae of these parameters are given. The IPCE is plotted as a function of the excitation wavelength, which is determined at 10 nm intervals from 400 to 800 nm:

$$\mathrm{IPCE} = \frac{1\,240\ I_{\mathrm{ph}}}{\lambda P_0} \tag{4}$$

where I_{ph} and P_0 are the photocurrent and the power of the incident radiation per unit area, respectively; and λ is the wavelength of the monochromatic light. No corrections are made for absorption and reflection in the substrate. For regenerative photoelectrochemical systems, V_{oc} is defined by

$$V_{\mathrm{oc}} = \frac{kT}{e}\ln\left(\frac{I_{\mathrm{inj}}}{n_{\mathrm{cb}}k_{\mathrm{et}}C_{\mathrm{I_3^-}}}\right) \tag{5}$$

where k is the Boltzmann constant; T is the absolute temperature; e is the quantity of electric charge; $C_{I_3^-}$ is the I_3^- concentration; I_{inj} is the flux of charge resulting from electron injection from the sensitizing dye; n_{cb} is the concentration of electrons at the TiO_2 surface; and k_{et} is the rate constant for I_3^- reduction by CB electrons. The fill factor and η are defined by

$$F_{\mathrm{F}} = \frac{V_{\max}I_{\max}}{V_{\mathrm{oc}}I_{\mathrm{sc}}} \tag{6}$$

$$\eta = \frac{V_{\mathrm{oc}}I_{\mathrm{sc}}F_{\mathrm{F}}}{P_{\mathrm{in}}} \times 100\% \tag{7}$$

Tab. 2 Photoelectrochemical data of the dye-sensitized solar cells based on ZnTCPc and N3

Sensitization	N3[6]	ZnTCPc	ZnTCPc/lauric acid
Abs/nm	530	688	688
IPCE/%	83	0.37	0.62
I_{sc}/(mA · cm^{-2})	18.2	0.147	0.163
V_{oc}/mV	720	277	289
F_F	0.73	0.51	0.56
η/%	10	0.021	0.026

where V_{max}, I_{max} and I_{sc} are the photovoltage, the photocurrent for maximum power output, and the short-circuit photocurrent, respectively; V_{oc} and P_{in} are the open-circuit photovoltage and the intensity of incident light.

The IPCE curves of the device based on ZnTCPc are shown in Fig. 5(a). The broad IPCE curve for ZnTCPc covers almost the near-IR region from 500 to 800 nm with a maximum of 0.37%. After the lauric acid is absorbed by the TiO_2 film electrodes, the corresponding IPCE values rise from 0.37% to 0.62% at 688 nm. Maybe the ZnTCPc aggregation is suppressed by the lauric acid membrane and then the aggregated filter effect becomes weak. The above factor improves I_{ph} values. Hence, both I_{sc} and η also grow from 0.147 to 0.163 mA/cm^2 and from 0.021% to 0.026%, correspondingly. While the visible region makes the main contribution to the high IPCE of N3, especially from 350 to 700 nm with a maximum of 83%. So the I_{sc} and η of N3-sensitized solar cells achieve 18.2 mA/cm^2 and 10%, respectively(see Tab. 2). Though the extinction coefficient of ZnTCPc ($\varepsilon_{\mathrm{ZnTCPc}} \approx 10^5$ mol/(L · cm) is close to

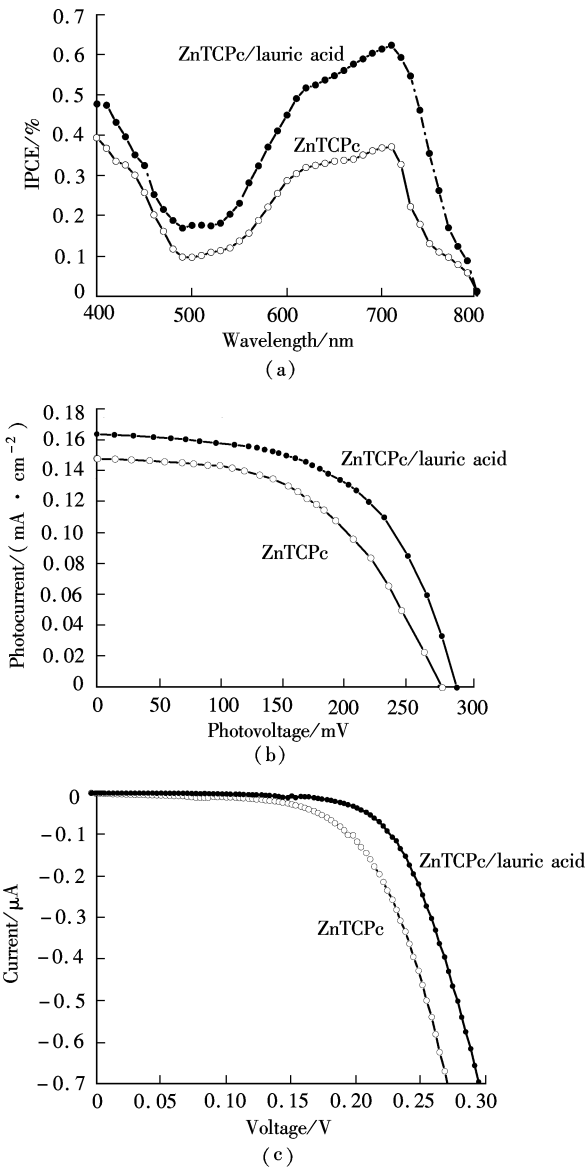

Fig. 5 Photovoltaic properties. (a) IPCE; (b) *I-V*; (c) Dark current

that of N3 ($\varepsilon_{N3} \approx 10^4$ mol/(L · cm), the ZnTCPc solubility ($C_{ZnTCPc} \approx 10^{-7}$ mol/L) is much poorer than the N3 solubility ($C_{N3} \approx 10^{-4}$ mol/L). Therefore, the light-harvesting yield of ZnTCPc is much lower than that of N3. At the same time, the zinc d levels do not lie between the ZnTCPc HOMO and LUMO orbitals according to the above experimental and theoretical suppositions. These facts directly result in a low electron-injection yield and then the IPCE values become correspondingly weak. The results indicate that ZnTCPc without higher electron acceptor groups results in slower and more ineffective electron injection from the LUMO to the CB of TiO_2 than that of Ru-dyes. When the sunlight is filtered through the aggregated ZnTCPc, the decreasing light-harvesting yield reduces the I_{inj} values. Simultaneously, the ZnTCPc symmetrical structure without electron releasing groups induces the intensive dark current, arising from the I_3^- reduction by the CB electrons at the TiO_2-I^-/I_3^- interface.

According to Eq. (5), the V_{oc} of the ZnTCPc cell and the ZnTCPc-lauric acid cell are 277 and 289 mV, as shown in Fig. 5(b). From the energy level distribution of Fig. 2(b), it is also known that V_{oc} is theoretically determined by the difference between the potential of the I^-/I_3^- redox couple (E_{redox}) and the quasi-Fermi level (E_f) of electrons in TiO_2 nanocrystalline under illumination as follows:

$$V_{oc} = | E_f - E_{redox} | \quad (8)$$

With the change in micro-environments, the positions of E_f and E_{redox} will change negatively. As for ZnTCPc and N3, the E_f position of the ZnTCPc is more positive than that of the N3, and the E_{redox} position of ZnTCPc is more negative than that of N3[13-14]. So the V_{oc} of the ZnTCPc-sensitized solar cell is lower than that of the N3-sensitized solar cell (720 mV). F_F is an important parameter, indicating the capacity of DSSC output power. In Fig. 5(c), the dark current of lauric acid assisting the ZnTCPc-sensitized solar cell (blue) is obviously restrained and the corresponding F_F increases from 0.51 to 0.56. After adding lauric acid, both aggregation and dark current decrease; η improves from 0.021% to 0.026%.

3 Conclusion

The following main factors may cause the performance of ZnTCPc-sensitized solar cells to be poor. First, the symmetrical structures of ZnTCPc lack releasing groups and anchoring groups. Secondly, the HOMO and LUMO of ZnTCPc divide the work indeterminately, that is to say, the HOMO location is not shared by both the zinc metal and the isoindoline ligands. The LUMO location does not obviously strengthen the interaction coupling between ZnTCPc and TiO_2. Compared with N3, the energy level distributions of ZnTCPc have disadvantages and the zinc d levels do not make a contribution to the MLCT process of ZnTCPc. Thirdly, the aggregation still exists in spite of adding lauric acid. Finally, the lifetime of excited ZnTCPc is much shorter than that of excited N3. So the oxidized dye has not enough time to accept electrons from the I^- redox mediator, regenerating the ground state.

References

[1] Baik C, Kim D, Kang M S, et al. Organic dyes with a novel anchoring group for dye-sensitized solar cell applications [J]. *J Photochem Photobiol A Chem*, 2009, **201**(2/3): 168 - 174.

[2] McCall K L, Jennings J R, Wang H X, et al. Novel ruthenium bipyridyl dyes with S-donor ligands and their application in dye-sensitized solar cells [J]. *J Photochem Photobiol A Chem*, 2009, **202**(2/3): 196 - 204.

[3] Grätzel M. Recent advances in sensitized mesoscopic solar cells [J]. *Acc Chem Res*, 2009, **42**(11): 1788 - 1798.

[4] Tian H N, Yang X, Chen R K, et al. Phenothiazine derivatives for efficient organic dye-sensitized solar cells [J]. *Chem Commun*, 2007, **36**: 3741 - 3743.

[5] He J J, Benkö G, Korodi F, et al. Modified phthalocyanines for efficient near-IR sensitization of nanostructured TiO_2 electrode [J]. *J Am Chem Soc*, 2002, **124**(17): 4922 - 4932.

[6] Chen C Y, Lu H, Wu C G, et al. New ruthenium complexes containing oligoalkylthiophene-substituted 1, 10-phenanthroline for nanocrystalline dye-sensitized solar cells [J]. *Adv Funct Mater*, 2007, **17**(1): 29 - 36.

[7] Lever A P, Pickens S R, Minor P C, et al. Charge-transfer spectra of metallophthalocyanines: correlation with electrode potentials [J]. *J Am Chem Soc*, 1981, **103**(23): 6800 - 6806.

[8] Yao Q H, Meng F S, Li F Y, et al. Photoelectric conversion properties of four novel carboxylated hemicyanine dyes on TiO_2 electrode [J]. *J Mater Chem*, 2003, **13**(5): 1048 - 1053.

[9] Giribabu L, Kumar C V, Reddy V G, et al. Unsymmetrical alkoxy zinc phthalocyanine for sensitization of nanocrystalline TiO_2 films[J]. *Sol Energy Mater Sol Cells*, 2007, **91**(17): 1611 - 1617.

[10] Tsaryova O. Darstellung und untersuchung der photochemischen und photosensibilisierenden eigenschaften verschieden substituierter Zn(Ⅱ)-Phthalocyanine [D]. Bremen, Germany: Universität Bremen, 2006.

[11] Hagfeldt A, Grätzel M. Molecular photovoltaics [J]. *Acc Chem Res*, 2000, **33**(5): 269 - 277.

[12] Kroops S E, Barnes P, Regan B, et al, Kinetic competition in a coumarin dye-sensitized solar cell: injection and recombination limitations upon device performance [J]. *J Phys Chem C*, 2010, **114**(17): 8054 - 8061.

[13] Ino D, Watanabe K, Takagi N, et al. Electron transfer dynamics from organic adsorbate to a semiconductor surface: zinc phthalocyanine on TiO_2(110) [J]. *J Phys Chem B*, 2005, **109**(38): 18018 - 18024.

[14] Gao W Y, Kahna A. Controlled p-doping of zinc phthalocyanine by coevaporation with tetrafluorotetracyanoquinodimethane: a direct and inverse photoemission study [J]. *Appl Phys Lett,* 2001, **79**(24): 4040 - 4042.

2,9,16,23-四羧基酞菁锌敏化太阳能电池中染料分子结构对电子转移的影响

王育乔[1] 崔 霞[1] 马艺文[1] 祁昊楠[1] 张慧君[1] 张 远[2] 孙岳明[1]

([1] 东南大学化学化工学院,南京 211189)
([2] 扬州大学化学化工学院,扬州 225002)

摘要:合成和表征了2,9,16,23-四羧基酞菁锌,并将其作为光敏染料应用于染料敏化太阳能电池.通过荧光光谱、循环伏安和量化计算等方法分析了该染料的激发态寿命、能级匹配和前线轨道分布等参数及其对电池性能的影响.结果表明:激发态寿命为0.1 ns,带隙为1.81 eV,HOMO分布未被锌原子和异二氢吲哚配体共享,LUMO分布不能增强染料与二氧化钛表面之间的相互作用;同时因酞菁类染料易聚集,因此所组装成的电池的短路电流密度为0.147 mA/cm^2,开路电压为277 mV,填充因子为0.51,效率为0.021%.

关键词:酞菁锌;太阳能电池;前线轨道;电子转移
中图分类号:O641.122;O626